International Journal of Microwave and Wireless Technologies

cambridge.org/mrf

A multi-function resonator based on an asymmetric tri-post rectangular waveguide section

Lyudmila P. Mospan[1,2] and Sergiy O. Steshenko[1]

[1]Computational Electromagnetics Lab., O.Ya. Usikov Institute for Radiophysics and Electronics of the National Academy of Sciences of Ukraine, Kharkiv, Ukraine and [2]Department of Ukrainian and Russian as foreign languages, O.M. Beketov National University of Urban Economy in Kharkiv, Kharkiv, Ukraine

Research Paper

Cite this article: Mospan LP, Steshenko SO (2020). A multi-function resonator based on an asymmetric tri-post rectangular waveguide section. *International Journal of Microwave and Wireless Technologies* **12**, 1005–1011. https://doi.org/10.1017/S1759078720000951

Received: 29 November 2019
Revised: 23 June 2020
Accepted: 24 June 2020
First published online: 22 July 2020

Key words:
Bandpass filters; poles and zeros; resonator filter

Author for correspondence:
Lyudmila P. Mospan;
Email: lyudmila.mospan@gmail.com

Abstract

A novel waveguide resonator is proposed in the paper. The resonator is composed of three rectangular partial-height posts inserted along a rectangular waveguide cross-section. A pair of lateral posts is mounted symmetrically whereas the third antipodal post is centered. The resonator enables bandreject, singlet-type, and pseudoelliptic responses. The operating regimes are achieved by a manipulation with the pair of lateral posts, namely by changing their heights or their locations in a waveguide cross-section. A filtering function is realized as the third mode is exploited as the resonant one. Measurement data are presented for WR90 waveguide. An explanation of the resonant phenomena in post-based sections in terms of eigen regimes and interacting oscillations is proposed.

Introduction

Generation of transmission zeros (TZs) in a frequency response is widely used in modern microwave engineering in order to design the filters that provide high selectivity or/and wider and deeper stopbands [1, 2]. It is highly desirable to generate a multi-pole response without increasing both transversal and longitudinal dimensions of a filter. Thus, a complication of the filter cross-section is required. It can be realized in different manners, in particular, by breaking the structure symmetry or (and) by implementing additional elements with (or without) modification of their profiles. Numerical and experimental data for some developed designs are presented in [3–10].

Thin post-based waveguide resonators with the posts inserted along a cross-section are good candidates for microwave filters as well. They are simple, compact, and allow for involving the higher modes into TZ generation. Post-based waveguide singlets have been reported recently in [11, 12]. Rectangular sections with two uneven posts inserted along a waveguide cross-section provided both a transmission pole (TP) and a TZ. Moreover, a sequence of the singlets acting as a doublet was reported in [11] as well. Later, a pseudoelliptic filter realized on the pairs of L–shaped inserts in a rectangular waveguide and in a substrate-integrated waveguide was reported in [13, 14]. In according to the nonresonating node approach proposed by Amari and Rosenberg [15, 16], a two-post-based resonator exploits the fundamental nonresonating mode bypass coupling from a source to a load in order to generate a TZ. The second mode was exploited as a resonant one in order to provide a filtering function. Breaking of the section symmetry is a mandatory condition as the second mode is not excited in a symmetric section.

A resonator of a different geometry is presented in the paper. It is a tri-post section. Its photographs and a schematic view are shown in Figs 1(a) and 1(b). The resonator utilizes the third mode (quasi-TE_{30}) in order to generate a filtering function. The basic idea of the resonator was proposed first in [17]. It was demonstrated that the third mode could be involved into a resonant interaction by a manipulation with the posts. In this paper, a breaking of the section symmetry is used in order to force the third mode be resonant. The symmetry breaking is realized by increasing the height of a lateral post and decreasing another one synchronously.

Besides, it is shown that the same responses can be generated keeping the section symmetry.

A symmetric equal-height post-based section enables three different responses as well. It is a separate impressive result of our study. From the other hand, this section is an intermediate stage in the way to the claimed asymmetric resonator. That is why a separate part of our paper is devoted to this section.

Finally, the aim of our paper is to present a new element enabling different responses, to carry out appropriate parametric study in order to demonstrate a transformation of the response, to reveal general dependencies and to investigate the reasons of revealed phenomena. A real filter design scheme accompanied by the circuit theory is out of the scope of the paper.

CAMBRIDGE UNIVERSITY PRESS

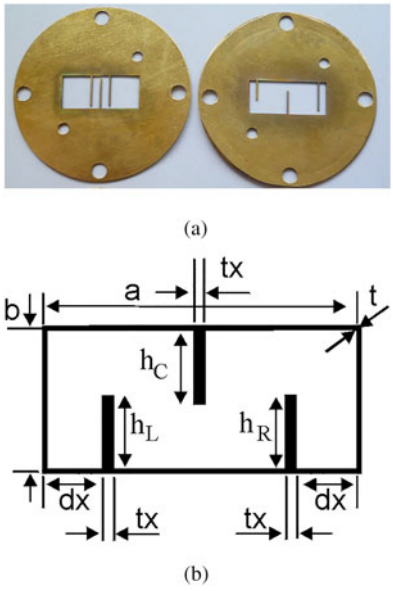

Fig. 1. Photograph of a symmetric and an asymmetric three-post based sections (a) and their schematic view (b).

An earlier version of this paper was presented at the first European Microwave Conference in Central Europe and was published in its Proceedings [18].

The resonator design and characteristics

Numerical calculations of the resonator scattering characteristics are obtained using home-made software MWD-II [19]. The software is based on the generalized scattering matrix technique and the mode-matching technique for the waveguides with piece-wise boundaries. All the calculations were carried out for a perfect conductor whereas the measurements are performed with the brass samples.

The section under consideration is constructed by three *E*–plane rectangular partial-height posts inserted along a rectangular waveguide cross-section of the width $a = 23$ mm and the height $b = 10$ mm. A pair of posts is mounted symmetrically whereas the third antipodal post is centered. Lateral posts are inserted along a waveguide cross-section at the distance dx from the waveguide side walls. Here, all three posts have rectangular footprints of the width $tx = 0.5$ mm and the thickness $t = 0.5$ mm. Centered post height $h_c = 7.2$ mm is fixed.

Symmetric resonator with equal-height posts

In contrast to known two-post resonators [12, 20], a distance between the posts is the parameter changing the frequency response drastically. As an illustration of a frequency response transformation, a parametric study with dx as a varying parameter is presented for the section with the posts of $h = h_{L,C,R} = 7.2$ mm height. The lateral posts of the starting configuration are located at the distance $dx = 2.0$ mm from the waveguide side walls. The simulated and the measured transmission characteristics of the section are plotted in Fig. 2(a). As it can be noticed from the figure, the section provides a bandstop frequency response with a single-standing transmission zero TZ_1 (marked by a down-oriented triangle ▼). Its measured frequency is $f(TZ_1) = 10.906$ GHz whereas the simulated frequency is $f(TZ_1) = 10.966$ GHz. Besides, an extremely high-quality singlet (TZ_2/TP) located at the lower frequencies is discovered in the simulations. Because of the Ohmic loss, a hump is detected at the measured response instead of the singlet pair TZ_2/TP.

Numerical investigations show that a simultaneous changing of the heights of all the posts is effective at controlling the transmission zero TZ_1 location. In the same manner as for a section with two identical posts [20], the shorter are the posts, the higher is the frequency of TZ. Compared to a dual-post design, a lower quality-factor reflection is achieved by using a three-post section.

A study of the transversal electric field distribution at the frequency of TZ_1 was performed in order to identify the mode dominating in the TZ generation. The field distribution at the frequency $f(TZ_1)$ is symmetric with one variation along the broad wall of the section. As it is pointed out in the section "A physical interpretation of the resonant phenomena in post-based sections," the section exploits the lowest (nonresonating) quasi-TE_{10} mode and the higher-order quasi-TE_{11} mode in order to generate the TZ. The second quasi-TE_{20} mode is antisymmetric with two field variations along the section broad wall. It is not excited in a symmetric structure. The third quasi-TE_{30} mode is symmetric. It participates in the singlet TZ_2/TP generation but it is almost decoupled with the load and the source. Thus, a filtering function is not provided.

A transformation of the frequency response begins when the distance dx reaches the value of $a/4$ approximately. As the distance dx grows, the transmission zero TZ_1 and the singlet TZ_2/TP shift up. A frequency separation between the pole TP and zero TZ_2 increases whereas the quality factors of the resonance (TP) and antiresonance (TZ_2) fall. As an example, the simulated frequency response of the section with $dx = 7.2$ mm is plotted in Fig. 2(b). The low-frequency transmission zero TZ_2 (marked by an upper-oriented triangle ▲) and the pole TP (marked by a circle ●) are observed clearly.

At a certain value of dx, a symmetric pseudoelliptic response is generated. Typical response of the section with $dx = 8.075$ mm is plotted in Fig. 2(c). The field distribution at the pole frequency f (TP) is symmetric and has three variations like one of the third mode. Thus, the resonator exploits third mode as a resonant one in order to provide a filtering function. The field distribution at the lower frequency zero TZ_2 has the similar character. Moreover, the field distribution at the higher frequency zero TZ_1 changes and it has three variations as well.

Furthermore, the lower frequency zero TZ_2 shifts down whereas the pole TP and zero TZ_1 form a singlet pair. A typical response is shown in Fig. 2(d).

Appropriate cumulative data are presented in Fig. 3 where the frequencies of two TZs and the pole are plotted by the solid lines and the cut-off frequencies of the first three modes plotted by the dashed lines.

In the case of symmetric pseudoelliptic frequency response ($dx = 8.075$ mm), the frequency separation between two poles is 1.5 GHz approximately. Two parameters dx and $h = h_{L,C,R}$ have to be changed in order to shift the response keeping the same frequency separation. Appropriate cumulative data are presented in Fig. 4. As an illustration, the measured and calculated pseudoelliptic responses of the resonator with $dx = 8.5$ mm and $h = h_{L,C,R} = 9.15$ mm, are plotted in the Fig. 5. Two TZs are located at $f(TZ_1) = 8.208$ GHz and $f(TZ_2) = 9.669$ GHz. The pole is located at $f(TP) = 8.909$ GHz with the measured insertion loss 0.46 dB. The field distributions at the frequencies of the lower frequency

https://doi.org/10.1017/S1759078720000951 Published online by Cambridge University Press

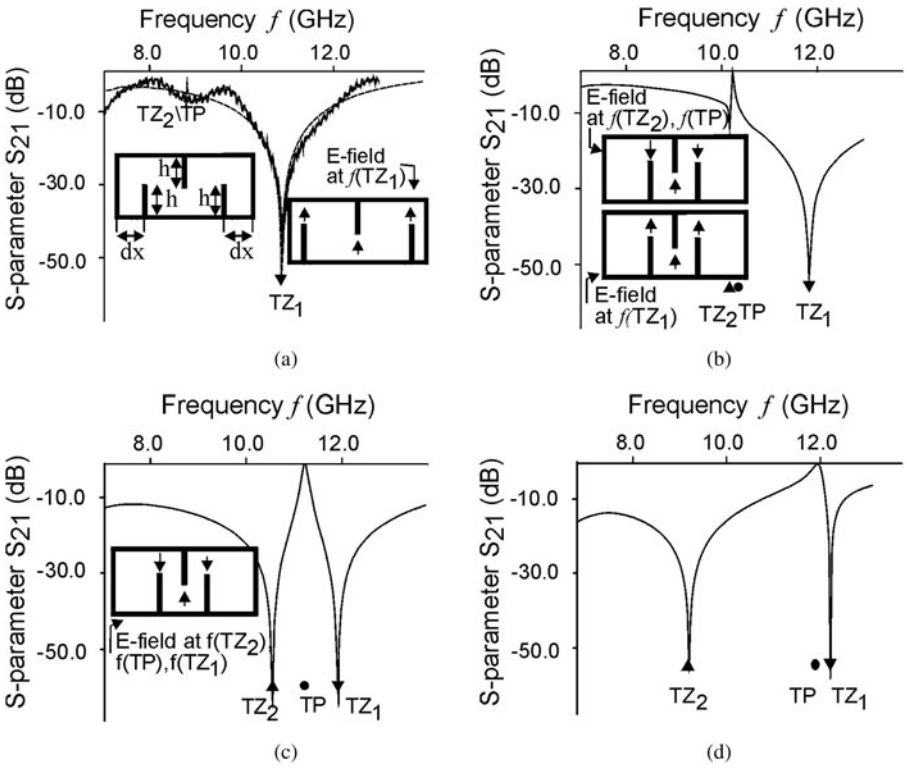

Fig. 2. Frequency responses of the resonator with equal height posts for different locations of the lateral posts: $dx = 2.0$ mm (a), 7.2 mm (b), 8.075 mm (c), 9.0 mm (d); and $h = h_{L,C,R} = 7.2$ mm. Electric field distributions in the middle cross-section of the resonator at the frequencies of TZ_1, TP, and TZ_2 are presented in the insets.

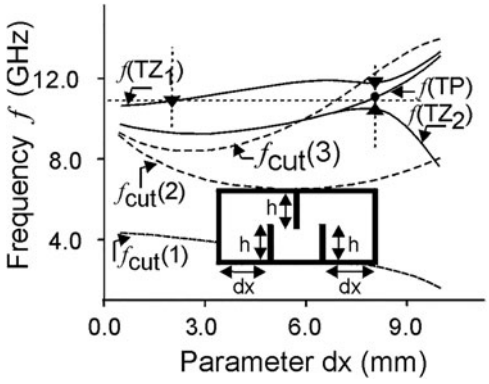

Fig. 3. Positioning of the TZs and TP by varying the locations of the lateral posts synchronously (dashed lines are the section cut-off frequencies). Data are presented for the symmetric resonator with equal-height posts: $h = h_{L,C,R} = 7.2$ mm.

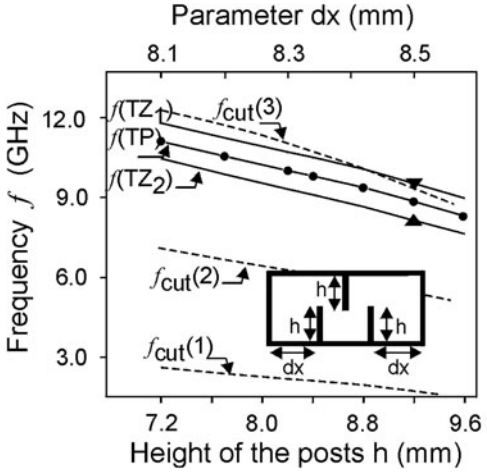

Fig. 4. Positioning of the TZs and TP by varying the heights $h = h_{L,C,R}$ of all the posts and the displacements dx of the lateral posts synchronously (dashed lines are the section cut-off frequencies). Data are presented for the symmetric resonator with equal-height posts.

zero TZ_2, the pole TP and the higher frequency zero TZ_1 keep three variations along the section broad walls.

Asymmetric resonator with unequal-height posts

Similar transformation of the response can be achieved by breaking the section symmetry. Here, the section symmetry breaking is realized by synchronous increasing the height of a lateral post and decreasing another one. As a result, a pseudoelliptic frequency response with two TZs located at both sides of the frequency of total matching is generated as well. Typical response for the case of $h_C = 7.2$ mm, $h_L = 8.55$ mm, and $h_R = 5.85$ mm, $dx = 2.0$ mm is plotted in Fig. 6. The TP frequency $f(TP)$ is 10.966 GHz and two TZs are located at $f(TZ_2) = 10.485$ GHz and $f(TZ_1) = 11.632$ GHz, respectively.

Note, the resonant frequency of the pseudoelliptic resonator is almost coincident with the frequency of total reflection of the incident TE_{10}-mode from the equal-post bandstop section. Thus, without applying an equivalent circuit a procedure of preliminary design of a pseudoelliptic prototype can be performed in two stages. First find the geometry of the equal-height three-post resonator whose response contains TZ located at the desired resonant frequency and adjust the lateral posts' heights synchronously to achieve desired pseudoelliptic filtering functions. Note, a frequency separation between TZs is controlled effectively by varying the offsets of the lateral posts in the range from 0 to

https://doi.org/10.1017/S1759078720000951 Published online by Cambridge University Press

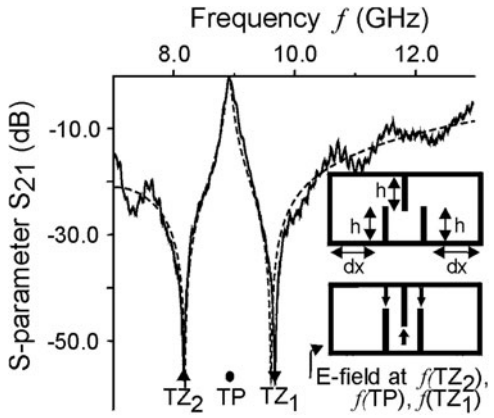

Fig. 5. Calculated and measured frequency responses of the symmetric resonator with closely spaced equal-height posts. Electric field distributions in the middle cross-section of the resonator at the frequencies of TZ_1, TP, and TZ_2 are presented in the insets.

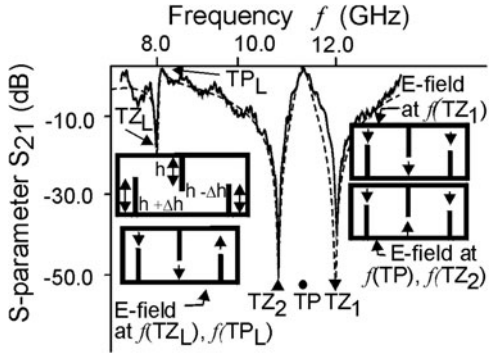

Fig. 6. Frequency responses of asymmetric tri-post resonator. Electric field distributions in the middle cross-section of the resonator at the frequencies of TZ_1, TP, and TZ_2 are presented in the insets.

$a/4$. Finally, apply an optimization procedure with obtained preliminary geometry.

A clear illustration of the frequency response transformation is obtained from a parametric study with Δh as a varying parameter. Appropriate cumulative data are presented in Fig. 7(a) where the frequencies of TZs and poles are plotted by solid lines and the cut-off frequencies of the second and the third modes plotted by dashed lines. A transformation of the frequency response begins as soon as the section symmetry is broken ($dh \neq 0$). It is seen from the figure that as Δh grows:

- Two singlet pairs TZ_L/TP_L and TZ_2/TP appear in the lower frequency range in the background of wideband TZ_1;
- The singlet pair TZ_L/TP_L shifts down. A frequency separation between its pole and zero is affected slightly;
- The resonant frequency $f(TP)$ of disturbed resonator shifts up linearly (and synchronously with the third mode cut-off frequency $f_{cut}(3)$) increasing over all the range of the varying parameter;
- Newly-appeared TZ frequency $f(TZ_2)$ shifts up having the TZ frequency $f(TZ_1)$ of the equal-post section as a limit (shown in Fig. 7(a)) by the triangle at the vertical axis. Similar behavior has been revealed early for the singlets implemented by a waveguide section with two uneven posts [20];

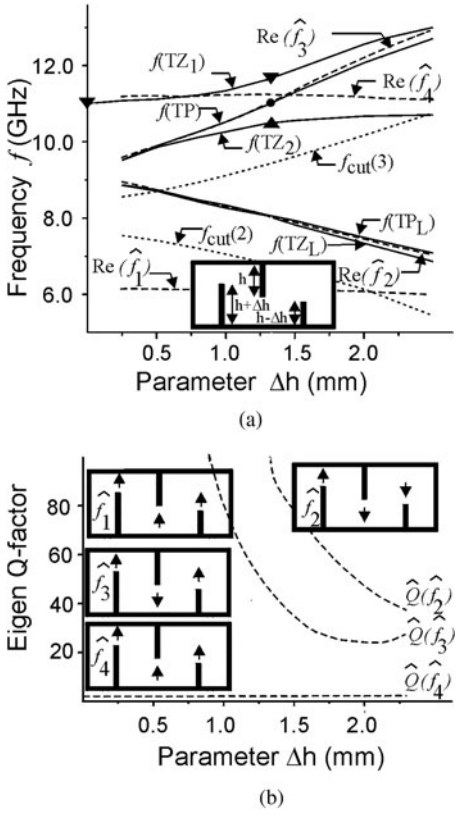

Fig. 7. Positioning of the TZs and TP by varying the heights of the lateral posts and a comparison with the natural regime characteristics $\hat{f}_{1,2,3,4}$ (dashed lines). Dotted lines are the section cut-off frequencies. Data are presented for the asymmetric resonator: $h_C = 7.2$ mm.

- The higher frequency TZ (TZ_1) is slightly affected at first and then shifts up. At a certain value of Δh, a pseudoelliptic response is generated whose pole frequency is equal to the rejection frequency of equal-post rejection section;
- Finally, TP and TZ_1 form a singlet pair.

A physical interpretation of the resonant phenomena in post-based sections

A physical explanation of the revealed transformation of the frequency response can be given in different ways. It can be a classical explanation based on an equivalent LC-circuit whose behavior is defined by a relation of its capacitive and inductive elements. Such an explanation has been used for example in [21] for multi-aperture waveguide irises. We have used a different approach while studying the multi-aperture irises [3, 22]. Resonant phenomena arising in the irises have been treated in terms of eigen regimes characterized by their natural oscillations. According to [23], all the frequency response of the waveguide unit may be restored by its eigen frequencies. The total transmission resonance generated by a classic one-aperture iris has been associated with the eigen regime characterized by one natural oscillation of complex frequency. The resonance frequency and the quality factor have been estimated by the values of the real and imaginary parts of one complex-valued frequency, respectively. Here, the complex-valued eigen frequency of natural oscillation excited in the waveguide resonator is the root of the

https://doi.org/10.1017/S1759078720000951 Published online by Cambridge University Press

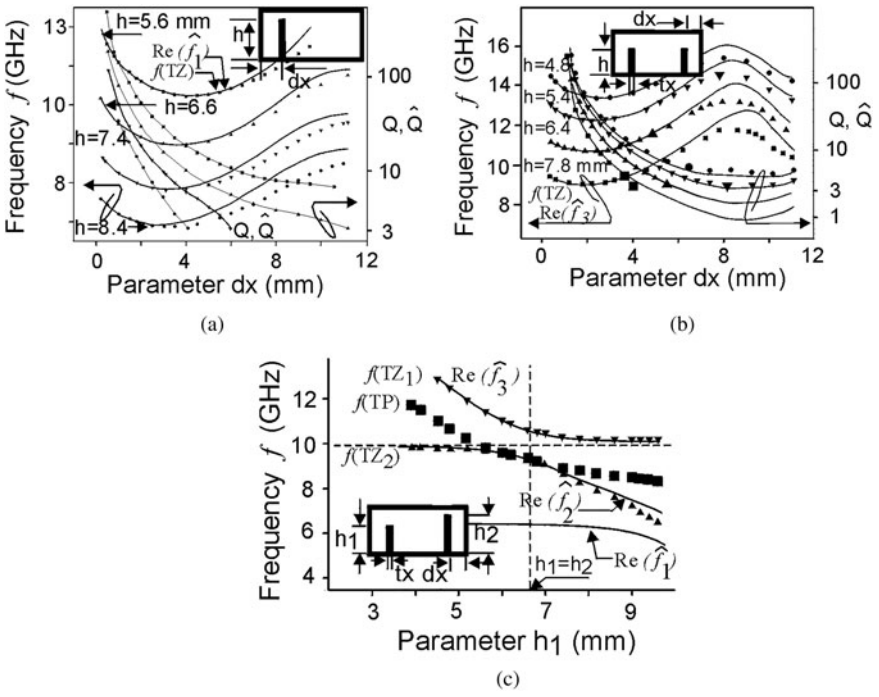

Fig. 8. A correlation between the scattering characteristics (frequencies of TZs and TP and quality factors) and the natural regime characteristics $\{\hat{f}_i\}$, $\{\hat{Q}_i\}$ for post-based sections.

homogeneous matrix equation $A(f)X = 0$ [24, 25] where $A(f)$ is an operator-function, X is a vector of unknown amplitudes. The homogeneous matrix equation is obtained from an inhomogeneous matrix equation$A(f)X = B$ (where B is the vector of the incident modes' amplitudes) of appropriate scattering problem by applying the radiation condition requiring the absence of the waves incident from infinity. Besides, it has been revealed in [3, 22] that cutting of additional slot(s) in a classic iris provided two paths for the input signal energy transfer from the input waveguide to the output one. Similarly to [26], a TZ was generated at a fixed frequency because of a destructive interference. The eigen regime of the two-iris is characterized by a couple of natural oscillations of complex frequencies. The TZ has been interpreted in [3, 22] as a response to the simultaneous excitation of a pair of natural oscillations. TZ frequency was close to the real part of the eigen frequency of high-quality natural oscillation.

Similarly to a multi-aperture iris, a thin post-based waveguide section can be considered as an iris and as a resonator of a specific type that provides a multi-path transfer as well. As shown in [27], the waveguide section with one off-centered post enables an implementation of one TZ known as a reflection resonance of quarter-wavelength post. Here, the two-path transfer is provided by the lowest (quasi-TE_{10}) and the first higher (quasi-TE_{20}) modes of the section. The lowest mode of a post-based section is identified in [11] as nonresonant one. No filtering function is generated because the lowest mode is operated far bellow its cutoff frequency and the second mode is coupled strongly with the dominant mode of the input and output waveguides. In our interpretation, a pair of natural oscillations is excited in the waveguide resonator. One of them is real-valued, bellow-cutoffand formed by the first mode . The second oscillation is a low-quality complex-valued one formed mostly by the second mode. TZ location and the bandwidth of the reflection resonance can be estimated by the values of the real and imaginary parts of the second oscillation frequency, respectively. Appropriate plots are shown in Fig. 8(a), where $Q = f(TZ)/\Delta f_{3\mathrm{dB}}$ is the quality factor of the reflection resonance (TZ). $\hat{Q} = -\mathrm{Re}\,(\hat{f}_2)/(2\mathrm{Im}\,(\hat{f}_2))$ is the natural oscillation quality factor, and $\hat{f}_2$ is the second natural oscillation frequency (both are plotted by solid lines). The section geometry: $a \times b = 23$ mm×10 mm, $t = 1$ mm, $tx = 0.5$ mm. It should note that the section generates the TZ even in the case of centered post. A low-quality TZ is located at the higher frequencies. The second mode is not excited in a symmetric unit and the second oscillation is formed mostly by a different higher mode of the section. Here, the second oscillation can be associated with quasi-TE_{11} mode of the section as its eigen frequency tends the cutoff frequency of $\boldsymbol{TE}_{11}$-mode of the rectangular waveguide if the centered post height tends zero.

A similar frequency response with a single broadband TZ is achieved by the help of a symmetric two-post section with two equal posts [20]. Again, TZ is interpreted as a response to the simultaneous excitation of a pair of natural oscillations. They are associated with the first and the third (quasi-TE_{30}) modes of the section. A correlation between the reflection resonance (TZ) location and the quality-factor obtained by the help of the scattering problem solution and corresponding eigen regime is plotted in Fig. 8(b), where $\hat{Q} = -\mathrm{Re}\,(\hat{f}_3)/(2\mathrm{Im}\,(\hat{f}_3))$ is the third natural oscillation quality factor and $\hat{f}_3$ is the third natural oscillation frequency. The section geometry: $a \times b = 23$ mm×10 mm, $t = 1$ mm, $tx = 0.5$ mm.

A two-post section with unequal posts provides a singlet-type frequency response [11, 12]. More exactly, a singlet pair of closely spaced TZ_2 and TP is generated in the background of another wideband TZ_1 (see plots in Fig. 8(c) [12]). The resonator filtering function is achieved owing to the second mode excited in the resonator because of the breaking of the section symmetry. The first (nonresonating quasi-TE_{10}) and the second (quasi-TE_{20}) modes participate in TZ_2 generation whereas the third (quasi-TE_{30}) and the first modes participate in TZ_1 generation. Within the concept of eigen regimes, the pair of the first and the second oscillations is responsible for generation of newly appeared TZ_2 whereas the first and the third oscillations together are responsible for the

https://doi.org/10.1017/S1759078720000951 Published online by Cambridge University Press

generation of TZ_1. We observe that two parametric curves of $\mathrm{Re}(\hat{f}_3)$ and $\mathrm{Re}(\hat{f}_2)$ draw a Vienne-type chart that is characteristic of the interacting oscillations (see, e.g. [24]). Responding to their eigen frequencies tend to come close but the interacting oscillations' curves never cross because the oscillations belong to the different groups of symmetry. A virtual distinction line is indicated by the horizontal dotted line. Besides, the parametric curves of $f(TZ_1)$ and $\mathrm{Re}\hat{f}_3$ are almost coincident over all the range of the geometrical parameter dx variation. The same is valid for the parametric curves of $f(TZ_2)$ and $\mathrm{Re}\hat{f}_2$. The parametric curve of $f(TP)$ is located between two hyperbolic curves of $f(TZ_1)$ and $f(TZ_2)$. Note such a behavior is inherent in an oversized waveguide resonator if its length is a varying parameter.

A tri-post based section was born in the complex plane $(\mathrm{Re}(\hat{f}), \mathrm{Im}(\hat{f}))$ as a result of above-mentioned studies. Thus, a pure mathematical approach gave birth for a new unit. A detailed mathematical background is presented in [17] in terms of natural oscillations for a three-post based section whose centered post is higher than two equal lateral posts.

Turning back to an equal-height tri-post section, an implementation of a single TZ_1 is caused by the simultaneous excitation of two natural oscillations as well. The pair consists of the first bellow-cutoff oscillation associated with the first (nonresonating quasi-TE_{10}) mode and the fourth oscillation associated with quasi-TE_{11} mode that belongs to the same group of the symmetry as the first one. The second oscillation is not excited. The third oscillation is extremely high-quality one. Its excitation results in the implementation of extremely high-quality pair TZ_2/TP shown in Fig. 2(a).

An asymmetric tri-post section exhibits more complicated operating regime. Four natural oscillations participate in the frequency response generation. The second mode is excited resulting in extremely high-quality TP_L generation. Together with the lowest mode, it participates in the extremely narrowband TZ_L implementation. It is very similar to the implementation of a singlet pair by a two-post section with unequal posts. In a similar manner, the third mode provides a resonant coupling resulting in the filtering function with the TP located at $f(TP)$. The first and third modes together implement TZ_2. Finally, TZ_1 is generated by the first and the fourth modes. A correlation between the frequencies of TZ_L, TP_L, TZ_2, TP, and TZ_1 and the section eigen regime is presented in Fig. 7(a) where the dashed curves of $\mathrm{Re}(\hat{f}_{2,3,4})$ are added. Besides, the parametric curves of the quality factors of $\hat{Q}_{2,3,4} = -\mathrm{Re}\,(\hat{f}_{2,3,4})/(2\mathrm{Im}\,(\hat{f}_{2,3,4}))$ of three natural oscillations are plotted in Fig. 7(b). $\hat{Q}_1$ is omitted as it tends infinity. It is seen from Fig. 7(a) that two parametric curves of $f(TZ_1)$ and $f(TZ_2)$ draw the Vienne-type chart around the crossed curves of real parts of the third and the fourth eigen frequencies. Thus, a coupling phenomenon takes place. Here, two interacting natural oscillations belong to the same symmetry group. Generally, two coupling regimes are available for the oscillations of the same symmetry, namely a continuation and a transformation [28]. Two oscillations are transformed into each other if their eigen frequencies come close in the transformation regime. It does not occur in the continuation regime. We deal with the continuation regime of the coupling between the third and the fourth natural oscillations of different qualities. Two parametric curves of $\mathrm{Re}(\hat{f}_3)$ and $\mathrm{Re}(\hat{f}_4)$ cross each other without a transformation of interacting oscillations. The continuation regime of interacting oscillations has been confirmed by studying the electric field distributions at the complex frequencies for the case of $dh = 1.0$, 1.35, and 1.8 mm. The field distributions have not transformed. Simplified distributions are shown in the insets in Fig. 7(b). They comply with the electric field distributions at real-valued frequencies $f(TZ_1)$ and $f(TZ_2)$. Besides, the electric field distribution at real-valued frequency $f(TP)$ is coincident with one at the complex valued frequency $\hat{f}_3$.

Conclusions

A novel simple and compact waveguide resonator is presented in the paper. It is composed of three rectangular partial-height posts inserted along a rectangular waveguide cross-section. A pair of posts is mounted symmetrically whereas the third antipodal post is centered.

The waveguide section acts as a bandreject element, a singlet, and a pseudoelliptic resonator. All the operating regimes are realized without any enlargement of the resonator dimensions. The operating regimes are achieved either by a breaking of the resonator symmetry or without it. Changing the lateral posts' locations in a resonator cross-section keeps the axis symmetry unchanged. Varying of the lateral posts' heights (namely increasing one of them and decreasing another one synchronously) breaks the resonator symmetry.

In contrast to known designs, the third mode exhibiting a symmetric electric field pattern is exploited as the resonant one.

An explanation of the resonant phenomena in post-based sections in terms of eigen regimes and a coupling inter oscillations is proposed.

References

1. **Hunter IC** (2001) *Theory and Design of Microwave Filters*. London, UK.: IEE Press.
2. **Kudsia CM Cameron RJ and Mansour RR** (2011) *Microwave filters for Communication Systems: Fundamentals, Design, and Applications*. New York, USA: Willey.
3. **Kirilenko AA and Mospan LP** (2000) Reflection resonances and natural oscillations of two-aperture iris in rectangular waveguide. *IEEE Transactions on Microwave Theory and Techniques* **48**, 1419–1421.
4. **Tomassoni C, Mongiardo M and Tarricone L** (2003) Analytical solution of scattering from multiple elliptical irises in rectangular waveguides. *AEU–International Journal of Electronics and Communications* **57**, 111–118.
5. **Don N, Kirilenko A and Mospan L** (2006) Layout of a multislot iris as a tool for the frequency response control. *Microwave and Optical and Technology Letters* **48**, 1472–1476.
6. **Kirilenko AA, Mospan LP and Tkachenko VI** (2002) Extracted-pole bandpass filters based on the slotted irises. *European Microwave Conference*, Milan, Italy.
7. **Ohira M, Deguchi H, Tsuji M and Shigesawa H** (2005) Novel waveguide filters with multiple attenuation poles using dual-behavior resonance of frequency-selective surfaces. *IEEE Transactions on Microwave Theory and Techniques* **53**, 3320–3326.
8. **Ohira M, Deguchi H, Tsuji M and Shigesawa H** (2005) A new dual-behaviour FSS resonator for waveguide filter with multiple attenuation poles. *European Microwave Conference*. Paris, France.
9. **Bage A and Das S** (2017) Stopband performance improvement of CSRR-loaded waveguide bandpass filters using asymmetric slot structures. *IEEE Microwave and Wireless Components Letters* **27**, 697–699.
10. **Bage A, Das S, Murmu L, Pattapu U and Biswal S** (2018) Waveguide bandpass filter with easily adjustable transmission zeros and 3-dB bandwidth. *International Journal of Electronics* **105**, 1170–1184.
11. **Tomassoni C and Sorrentino R** (2013) A new class of pseudoelliptic waveguide filters using dual-post resonators. *IEEE Transactions on Microwave Theory and Techniques* **61**, 2332–2339.

https://doi.org/10.1017/S1759078720000951 Published online by Cambridge University Press

12. **Mospan L, Prikolotin S and Kirilenko A** (2013) Singlet formed by two transversal ridges in a rectangular waveguide from the spectral theory point of view. *European Microwave Conference*, Nuremberg. Germany.
13. **Zemlyakov VV and Zargano GF** (2015) The novel compact microwave SIW filter based on L-ridged rectangular waveguide. *Journal of Electromagnetic Waves and Applications* **29**, 1699–1707.
14. **Zemlyakov V, Krutiev S, Tyaglov M and Shevchenko V** (2018) A design of waveguide elliptic filter based on resonant diaphragms with a complex aperture. *International Journal on Circuit Theory and Applications* **46**, 1–10.
15. **Amari S, Rosenberg U and Bornemann J** (2004) Singlets, cascaded singlets and the nonresonating node model for modular design of advanced microwave filters. *IEEE Microwave Wireless Components Letters* **14**, 237–239.
16. **Amari S and Rosenberg U** (2005) Characteristics of cross (bypass) coupling through higher/lower order modes and their application in elliptic filter design. *IEEE Transactions on Microwave Theory and Techniques* **53**, 3135–3141.
17. **Mospan L, Prikolotin S and Kirilenko A** (2016) Involving the higher modes into attenuation pole generation. *Spectral approach*, 9th International Kharkiv Symposium on Physics and Engineering of Microwaves, MM and SubMM Waves, Kharkiv, Ukraine.
18. **Mospan L and Steshenko A** (2019) A multi-function resonator based on an asymmetric tri-post rectangular waveguide section. *European Microwave Conference in Central Europe EuMCE*, Prague. Czech Republic.
19. **Prikolotin SA, Steshenko SA, Kulik DY, Rud LA and Kirilenko AA** (2012) Fast full 3D EM CAD of waveguide units based on the generalized mode-matching technique. *International Conference on MMET*, Kharkov. Ukraine.
20. **Kirilenko A, Kulik D, Mospan L and Rud' L** (2008) Two notched band two post waveguide. *12th International Conference on MMET*, Odessa, Ukraine.
21. **Leal-Sevillano CA, Montejo-Garai JR, Ruiz-Cruz JA and Rebollar JM** (2016) Wideband equivalent circuit for multi-aperture multi-resonant waveguide irises. *IEEE Transactions on Microwave Theory and Techniques* **64**, 724–732.
22. **Kyrylenko A and Mospan L** (2001) Two- and three-slot irises as bandstop filter sections. *Microwave and Optical Technology Letters* **28**, 282–284.
23. **Kirilenko AA and Tysik BG** (1993) Connection of S-matrix of waveguide and periodical structures with complex frequency spectrum. *Electromagnetics* **13**, 301–318.
24. **Sirenko YK and Ström S** (eds) (2010) *Modern Theory of Gratings: Resonant Scattering: Analysis Techniques and Phenomena*. New York: Springer-Verlag, p. 390.
25. **Shestopalov V and Shestopalov Y** (1996) *Spectral Theory and Excitation of Open Structures*. London: Peter Peregrinus.
26. **Jarry P, Gugliemi M, Kerherve E, Pham JM, Roquebrum O and Schmitt D** (2005) Synthesis of dual-mode in-line microwave rectangular filters with higher modes. *International Journal of RF and Microwave Computer-Aided Engineering* **15**, 241–248.
27. **Rosenberg U and Amari S** (2007) A novel band-reject element for pseudoelliptic bandstop filters. *IEEE Transactions on Microwave Theory and Techniques* **55**, 742–746.
28. **Yakovlev AV and Hanson W** (1998) Analysis of mode coupling on guided-wave structures using Morse critical points. *IEEE Transactions on Microwave Theory and Techniques* **46**, 966–974.

Lyudmila P. Mospan (IEEE SM'11) received her M.S. degree in radio engineering from the Kharkov State University, Kharkov, Ukraine, and her Ph.D. degree in radio engineering from the Institute of Radiophysics and Electronics of the National Academy of Sciences of Ukraine (IRE NASU), Kharkov, Ukraine, in 2001. She is currently a Senior Researcher in the Computational Electromagnetics Lab. of IRE NASU and an Associate Professor at O.M. Beketov National University of Urban Economy in Kharkiv, Kharkiv, Ukraine. Her research is focused on microwave computer-aided design and resonance phenomena in waveguides and gratings.

Sergiy O. Steshen received his M.S. degree in applied mathematics from Kharkiv National University (KhNU), Kharkiv, Ukraine, and his Ph.D. degree in radiophysics from the Institute of Radiophysics and Electronics of the National Academy of Sciences of Ukraine (IRE NASU), Kharkiv, Ukraine, in 1996 and 2006, respectively. From 2001 to 2005, he was with the Department of Mathematics, Kharkiv National University, as a Junior Scientist. From 2007 to 2008 and in 2010, he was a Postdoctoral Fellow with the Department of Information Engineering, University of Siena, Siena, Italy. He is currently Head of the Laboratory of Computational Electromagnetics, IRE NASU. His research interests include numerical methods for the analysis and design of waveguides and antennas, and eigenvalue problems.

https://doi.org/10.1017/S1759078720000951 Published online by Cambridge University Press